IEEE INFOCOM 2022 - IEEE Conference on Computer Communications Workshops (INFOCOM WKSHPS) | 978-1-6654-0926-1/22/$31.00 ©2022 IEEE | DOI: 10.1109/INFOCOMWKSHPS54753.2022.9798023

Heterogeneous Airborne mmWave Cells: Optimal Placement for Power-Efficient Maximum Coverage

Nima Namvar*, Fatemeh Afghah†
*School of Informatics, Computing and Cyber Systems, Northern Arizona University, Flagstaff, AZ, USA
Email:nima.namvar@nau.edu
† Electrical and Computer Engineering Department, Clemson University, 433 Calhoun Dr, Clemson, SC 29634, USA,
Email: fafghah@clemson.edu

***Abstract*—The flexible altitude of unmanned aerial vehicles (UAVs)-mounted base stations (BSs) and their higher chance of establishing a line-of-sight (LOS) link towards ground users, make them an appealing solution for outdoor mmWave communication. However, the positioning of UAVs is a critical problem that affects both the coverage performance and energy consumption. In this work, considering a heterogeneous set of UAVs acting as aerial mmWave BSs, we develop an effective approach for the 3D positioning of the UAVs that leads to maximum coverage area with minimal power consumption. The UAVs have a varying transmit power and flight altitude range. Given a repository of UAVs, the proposed method finds an optimal subset of the available UAVs and determines their 3D position for maximum LOS coverage area with minimum energy consumption. First, we formulate an optimization problem to find the best subset of available UAVs along with their horizontal position. Next, we optimize the altitude of the UAVs based on the practical data of the geographical environment, such as the number and location of the buildings and other structures. Simulation results demonstrate the effectiveness of the proposed solution and provide valuable insights into the performance of the heterogeneous UAV-supported small cell networks.**

***Index Terms*—Unmanned Aerial Vehicle (UAV), mmWave signaling, LOS coverage maximization, constrained circle packing.**

I. Introduction

The 5G NR networks are progressively adopting the mmWave band (30-300 GHz) as a promising solution to cope with the steady proliferation of bandwidth-intensive devices and applications [1]. However, despite offering an extremely wide spectrum, the mmWave channels suffer from poor propagation characteristics. Channel measurements using directional antennas have revealed that mmWave signals are highly susceptible to blockage and thus, the channel power would arrive at the user mainly through the line-of-sight (LOS) path [2]. Furthermore, the excessive pathloss caused by the mmWave multi-gigahertz frequencies limits the scope of mmWave signaling to *short-range and LOS links*. These difficulties have been halting the ubiquitous implementation of mmWave signaling for outdoor applications since stationary and moving obstacles can potentially block the signals.

Meanwhile, the use of UAVs as flying base stations (BSs) to increase the network capacity has been the subject of neoteric and concerted research [3]. The UAV-mounted base stations (UAV-BSs) can be quickly deployed to provide on-demand wireless coverage and support the terrestrial network [4], [5]. More importantly, thanks to their mobility and adjustable altitude, the UAV-BSs possess a much higher likelihood of LOS connections towards the ground users [6]. Thus, if properly deployed and organized, the UAV-BSs offer an effective solution for outdoor mmWave signaling by establishing and maintaining LOS channels towards the users.

The UAV-assisted wireless networks encounter unique design challenges due to the altitude dimension and the mobility of the aerial BSs. In particular, the 3D deployment of the UAVs is arguably the most influential design consideration as it directly impacts the coverage, quality-of-service (QoS), and energy consumption of the network [5]. The works in [7], [8] investigated the optimal altitude of a single UAV operating under different fading assumptions. The authors in [9], [10] extended the previous results to the case of two or multiple identical UAV-BSs having the same transmit power and altitude. In [11], a UAV-enabled small cell placement problem is investigated in the presence of a terrestrial wireless network to maximize the number of covered users. Furthermore, the authors in [12] proposed a deployment plan to minimize the number of UAVs required for serving a certain number of ground users. Similar works can be found in [13]–[18].

While these studies address important UAV deployment scenarios, they implicitly assume that the UAVs are operating on microwave frequencies and do not consider unique features of mmWave channels in the deployment problem. Indeed, only a handful of recent works exist on the integration of UAV-assisted wireless networks and mmWave communications [19]–[23]. Furthermore, the aforementioned works mainly limit their discussions to cases in which there exists only a single UAV or multiple identical UAVs with the same capabilities. In practice, however, one might have a repository of various types of drones with diverse capabilities in terms of flight altitude range and transmit power. In this context, the exact number and the type of UAVs that need to be deployed depend on the environmental factors of the target area such as the number and distribution of the obstacles.

The main contribution of this paper is to develop a practical and efficient deployment technique for UAV-assisted mmWave networks to maximize their total downlink coverage area. Given a heterogeneous set of UAVs with varying transmit powers and flight altitude ranges, we jointly optimize the number and the type of required UAVs as well as their

3D position to maximize the coverage area with minimal energy consumption. In order to solve the optimal deployment problem, we divide it into two sub-problems. First, considering the *statistical model* of obstacles in the area, we formulate an optimization to select a subset of available UAVs and determine their horizontal location to maximize their total *raw coverage area*. Next, considering the exact locations and dimensions of the obstacles in the environment, we optimize the altitude of each selected UAV to maximize its *actual LOS coverage area* within which, the users may have seamless mmWave connectivity. The advantage of the proposed method is that rather than deploying all available UAVs, we use as many UAVs as needed to provide the network coverage while maintaining the desired QoS. In fact, the number and the type of selected UAVs are the design factors to be determined based on the size and shape of the area of interest. Moreover, we show that the proposed method has a polynomial time complexity which translates into good scalability.

The rest of this paper is organized as follows. The system model is described in Section II. The selection of UAVs and their optimal horizontal placement is discussed in Section III. The altitude optimization for maximum mmWave coverage is presented in Section IV. The simulation results are provided in Section V while the conclusions are drawn in Section VI.

II. System Model

The UAVs are equipped with mmWave communication to deliver high data rates on the downlink. Suppose that UAVs are of grouped into different classes depending on their maximum transmit power and flight altitude range. Let $\mathcal{U} = \{U_i\}_{i=1}^N$ denote the set of N available UAVs in the repository while P_i^t represents the transmit power of UAV U_i. The goal is jointly allocate and distribute the available resources, i.e., the UAVs, to service a given geographical area. By the *allocation of resources*, we mean selecting an optimal subset of the available UAVs to be deployed in the area. Further, by the *distribution of resources*, we mean the optimal placement of the UAVs to provide maximum wireless coverage.

Selecting the proper AtG channel model is the crucial step in formulating the DBS placement problem. In this work, we adopt the model presented in the seminal work [24]. The ground stations receive the signal from a UAV through two main paths; namely, the LOS path or strong non-LOS (NLOS) path caused by the reflectors in the environment. These two propagation groups occur with different probabilities depending on the density and the location of obstacles (e.g., buildings) relative to the position of the UAV.

In addition to the free space pathloss (FSPL), the radio signals emitted by a UAV-BS incur a random attenuation due to their propagation group. The total pathloss for an ATG channel is given by [8],

$$\Psi = 20\log\big(\frac{4\pi f_c d}{c}\big) + \eta_\xi, \tag{1}$$

in which f_c is the carrier frequency, c is the speed of light, d is the distance between the UAV and the ground user. The first term in (1) accounts for the FSPL while the second term, η_ξ, is a random variable that represents the excessive loss due to shadowing and scattering. Depending on whether the signal is received through LOS or NLOS paths, η_ξ takes on two values, i.e., η_{LOS} and η_{NLOS} with respective probabilities $\mathbf{P}_{\text{LOS}}$ and $\mathbf{P}_{\text{NLOS}} = 1 - \mathbf{P}_{\text{LOS}}$. The values of η_{LOS} and η_{NLOS} should be found experimentally and η_{NLOS} is typically much larger than η_{LOS}. The probability of LOS link is given by: [24]:

$$\mathbf{P}_{\text{LOS}}(\theta) = \frac{1}{1+\alpha\exp\left(-\beta(\theta-\alpha)\right)}, \tag{2}$$

in which $\theta = \arctan(\frac{h}{r})$ is the elevation angle for a UAV hovering at altitude h, measured from a user's location at horizontal distance r. The parameters α and β depend on the location, dimension, and distribution of the buildings and are determined based on the environment's statistical data. The probability of NLOS is $\mathbf{P}_{\text{NLOS}} = 1 - \mathbf{P}_{\text{LOS}}$. In this work, we use the spatial mean of pathloss, i.e., the expected value of pathloss over all propagation groups. Indeed, as we are concerned with the deployment of stationary UAV-BSs, we omit the multipath fading for simplicity. The expected pathloss is thus written as:

$$\overline{\Psi} = \text{FSPL} + \eta_{\text{LOS}}\mathbf{P}_{\text{LOS}} + \eta_{\text{NLOS}}\mathbf{P}_{\text{NLOS}}. \tag{3}$$

By substituting (1) and (2) into (3), and letting $d = \sqrt{h^2+r^2}$ to be the distance between a UAV at altitude h from a user located at radial distance r, we have,

$$\overline{\Psi} = 20\log(d) + \frac{A}{1+\alpha\exp(-\beta(\theta-\alpha))} + B, \tag{4}$$

in which $A = \eta_{\text{LOS}} - \eta_{\text{NLOS}}$ and $B = \eta_{\text{NLOS}} + 20\log(\frac{4\pi f_c}{c})$.

III. Horizontal Placement of UAVs for Maximum Raw Coverage Area

In this section, given the heterogeneous repository of UAVs, we jointly optimize the selection of UAVs as well as their horizontal location to maximize their aggregate coverage area. We employ the statistical ATG channel model presented in the previous section to optimize the horizontal placement of the UAVs. As the resulting coverage area is obtained from the statistical model of the environment and does not account for the exact realization of obstacles in the environment, we call it the *raw* coverage area. However, the exact location of the buildings and obstacles can greatly impact the mmWave channels. The key advantage of airborne BSs over their terrestrial counterparts is their adjustable altitude which adds an extra degree of freedom to system design. In the next section, we utilize this degree of freedom to optimize the altitude of the UAVs based on the exact distribution of the obstacles in the area to maximize the mmWave coverage area.

Definition 1: The raw coverage radius of a UAV with transmit power P^t hovering at altitude h is the maximum radial distance r from the UAV within which the received signal power $P^r = P^t - \overline{\Psi}$ is above a certain threshold ϵ, i.e., $R \triangleq \arg[P^r(r) = \epsilon]$.

By substituting (3) in the definition above and setting the partial derivative $\frac{\partial P^r}{\partial r} = 0$, the value of R is determined for each UAV depending on its transmit power and flight altitude. Usually, there is no closed-form solution to this equation and we need to resort to numerical methods to find the value of R.

Given the raw coverage radii of the UAVs in the repository, we will find the best subset of the available UAVs as well as their horizontal location to maximize the total raw coverage area. Without loss of generality, we consider the operation area to be a rectangle with length L and width W. Let (x_i, y_i, h_i) denote the location of UAV i should it gets selected for deployment. We formulate the following optimization problem:

$$\underset{I_i, x_i, y_i}{\text{maximize}} \quad \sum_{i=1}^{N} I_i \left(\pi R_i^2 - \vartheta P_i^t \right), \tag{5}$$

s.t.

$$I_i \in \{0, 1\}, \qquad i \in \{1, 2, \cdots, N\} \tag{6}$$

$$-\frac{W}{2} + R_i \leq x_i \leq \frac{W}{2} - R_i, \quad i \in \{1, 2, \cdots, N\} | I_i = 1 \tag{7}$$

$$-\frac{L}{2} + R_i \leq y_i \leq \frac{L}{2} - R_i, \quad i \in \{1, 2, \cdots, N\} | I_i = 1 \tag{8}$$

$$\sqrt{(x_i - x_j)^2 + (y_i - y_j)^2} \geq R_i + R_j, \quad i, j \in \{1, 2, \cdots, N\} | i \neq j, I_i = I_j = 1. \tag{9}$$

where N is the total number of available UAVs in the repository. In addition, I_i is an indicator function which equals to 1 if UAV $U_i \in \mathcal{U}$ is selected for covering the region and equals to 0 otherwise. It governs the resource allocation strategy for a given area of interest. Moreover, in (5), ϑ is the weighting factor, where setting $\vartheta = 0$ results in coverage maximization problem without considering energy efficiency. The objective function in (5) makes a trade-off between the covered area and the total transmission power. The constraint in (6) states that the indicator function can only take on 0 and 1 while constraints in (7) and (8) ensure that the coverage circle of UAV U_i with radius R_i does not extend outside the rectangular area. Finally, the constraint in (9) avoids any coverage overlap between the cells to reduce the risk of interference between neighboring cells.

The optimization problem stated in (5)-(9) is very challenging to solve. This challenge stems from the non-convexity of the objective function and the non-linearity of the constraints, as well as the high number of unknowns parameters. In its simplest form where the indicator function I_i is given $\forall i$ and all the UAVs have the same transmit power (i.e., homogeneous network), the proposed problem can be solved using the standard *circle packing (CP)* algorithms [25]. In the CP problem, the task is to arrange a given number of circles, say K circles on a surface such that no overlapping occurs. The goal is to maximize the packing density, which is defined as the proportion of the surface covered by the circles. The problem is known to be NP-hard [25]. Following the concept of *reduction* in algorithm design, we infer that the proposed optimization is also NP-hard.

A. Proposed Algorithm

Let $[-\frac{W}{2}, -\frac{L}{2}]$, $[\frac{W}{2}, -\frac{L}{2}]$, $[\frac{W}{2}, \frac{L}{2}]$, and $[-\frac{W}{2}, \frac{L}{2}]$ be the coordinates of the rectangular area in the 2D Cartesian plane. Assuming that there are already some disks fitted in the rectangular area we define the locus of the center (LoC) for a coverage disk as follows:

Definition 2: Consider a rectangle with length L and width W within which there exists a set of circles $\mathcal{C}$ satisfying the conditions stated in (7), (8), and (9). The LoC_i for a coverage disk with radius R_i is the set of all points (x_i, y_i) at which its center can be placed while all the conditions in (7), (8), and (9) are still satisfied. Formally,

$$\begin{aligned} \text{LoC}_i = \{(x_i, y_i) \big| \mid x_i \mid \leq \mid \frac{W}{2} - R_i \mid, \mid y_i \mid \leq \mid \frac{L}{2} - R_i \mid, \\ \sqrt{(x_i - x_j)^2 + (y_i - y_j)^2} \geq R_i + R_j, \\ \forall j \in \mathcal{C}, I_j = 1\}. \end{aligned} \tag{10}$$

Given a permutation ϕ of the coverage disks, the proposed algorithm places the disks at the lower leftmost possible position to maximize the density of disks while avoiding any overlap between the adjacent disks. In order to do so, we need to find the LoC for each new coverage disk that is appended to the existing fitted disks. For instance, the LoC_1 for the first circle with radius $\phi(R_1)$ is a smaller rectangle inside the rectangular surface with its edges having a distance $\phi(R_1)$ from the boundaries. If LoC_1 is not an empty set, the algorithm places the center of the first circle on the lower left-most corner of the LoC_1 and flags its corresponding indicator function. If the LoC_1 is empty, the algorithm assigns 0 to the corresponding indicator function, removes the circle R_1 from the list, and proceeds to the next circle in ϕ. Having already placed k circles in the desired surface, for the $(k+1)$th circle with radius R_{k+1}, we first compute the LoC_{k+1}. Then, if $\text{LoC}_{k+1} \neq \emptyset$, we select the lower left-most point on the LoC_{k+1} to place the circle. If the locus is empty, i.e., $\text{LoC}_{k+1} = \emptyset$, then it is not possible to insert the circle according to the mentioned constraints. Consequently, the algorithm removes all the remaining circles with the same size from the ordered tuple ϕ and proceeds to the next circle in the list. It stops when there are no more circles remaining in the list. Finally, the algorithm produces two subsets of ϕ: (a) a subset S of the disks that are placed into the area, and (b) a subset U of the disks that cannot be fitted in the area. The pseudocode for the proposed algorithm is provided in Algorithm 1. Once the solution for a particular permutation of disks is found, we can find the optimal solution by comparing the results for all the permutations.

Complexity Analysis: The overall complexity of the proposed algorithm mainly depends on calculating the LoC_i, i.e., the locus of center for circle $\phi(R_i)$. For $i = 1$, the computation of LoC_1 is trivial. For $i \geq 2$, the computation of LoC_i requires solving at most $\binom{i-1}{2} + 4(i-1)$ quadratic equations. Having computed LoC_i, if $\text{LoC}_i \neq \emptyset$ we select the lower leftmost intersection point as the center of $\phi(R_i)$ and proceed to the

Algorithm 1: Horizontal Placement of UAVs

Data: $\Phi = [\phi(R_1), \phi(R_2), \dots, \phi(R_N)]$ and the dimensions of rectangle $[W, L]$

Result: A feasible solution to the optimization problem in (5)-(9)

1 **Initialization:** $S \leftarrow \emptyset$ and $U \leftarrow \emptyset$
2 **for** $i \leftarrow 1$ **to** N **do**
3   **if** $\phi(R_i) \notin U$ **then**
4   Compute LoC_i
5   **if** $\mathrm{LoC}_i \neq \emptyset$ **then**
6   Find (a_i, b_i), the lower leftmost point on LoC_i
7       $(x_i, y_i) \leftarrow (a_i, b_i)$
8       $I_i \leftarrow 1$
9   Append $\phi(R_i)$ to S
10   **else**
11   **for** $j \leftarrow i$ **to** N **do**
12   **if** $\phi(R_j) = \phi(R_i)$ **then**
13   Append $\phi(R_j)$ to U
14           $I_j \leftarrow 0$
15   **end**
16   **end**
17   **end**
18   **else**
19   **continue**
20   **end**
21 **end**
22 **return** *S and U*

next circle in the list (lines 5 to 9 of Algorithm 1). However, if $\mathrm{LoC}_i = \emptyset$, we add the circle $\phi(R_i)$ and all the remaining circles with the same radius to the list U in order to prevent repeated calculations for similar circles that cannot be fitted into the rectangle (lines 11 to 16 of Algorithm 1). In the worst case scenario, we have $\mathrm{LoC}_i \neq \emptyset$ for all i and the algorithm calculates LoC_i for all circles, as stated in lines 5 to 10. In addition to finding LoC_i, there are two "assignment" functions in lines 7 and 8 and an "append" function in line 9 which are of $\mathcal{O}(1)$ complexity. Moreover, the "find" function in line 6 is of linear complexity over a list of $2\binom{i-1}{2}$ intersection points. Thus, the lines 5 to 10 require $2\binom{i-1}{2} + 3$ operations in each iteration. The total number of operations is given by:

$$\sum_{i=2}^{N} \left[(2i+1)\binom{i-1}{2} + 4i - 1\right] = \sum_{i=2}^{N} \left[i^3 - \frac{5}{2}i^2 + \frac{9}{2}i\right] = \frac{1}{4}N^4 + g(N), \tag{11}$$

where $g(N)$ is a polynomial of degree 3. Thus, assuming that the quadratic equations can be solved in constant time, the complexity of the proposed algorithm can be written as $\mathcal{O}(N^4)$. It can be seen that the algorithm has a polynomial time complexity which translates into a good scalability.

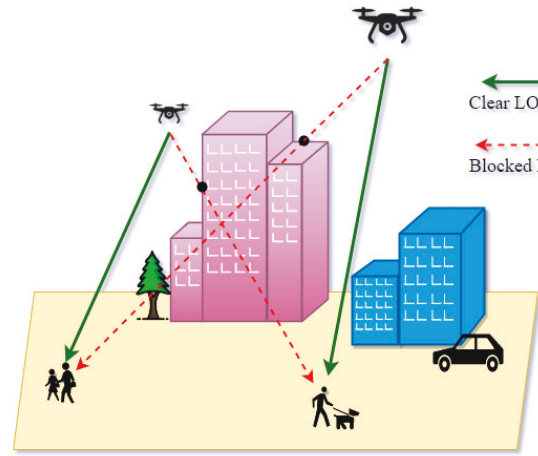

Fig. 1: LOS and NLOS links in UAV-assited mmWave system

IV. Vertical Placement of UAVs for Maximum LOS Visibility

Given the horizontal location of the UAVs, in this section we derive the optimal altitude for a UAV to maximize the actual mmWave coverage area of each single UAV. Since mmWave signaling is susceptible to blockage, it is necessary to establish secure LoS links between the UAVs and users for successful communications.

Assume that a UAV is located at altitude h_0 above the origin with cylindrical coordinates $(z, r, \phi) = (h_0, 0, 0)$ where z denotes the altitude coordinate, r is the radial distance from the z-axis, and ϕ is the azimuth angle. Considering a generic point on the ground located at $P = (0, r_0, \phi_0)$, we investigate whether it has a clear LOS view towards the UAV or the LOS view is blocked by buildings, as shown in Figure 1. We utilize the digital terrain model (DTM) which is a 3D computer generated model of elevation data for representing the terrain in an area. The DTM data provides the exact location and dimension of the environmental obstacles, which is crucial for mmWave cell planning. As shown in Figure 1, consider the virtual LOS line connecting a UAV and a generic point P on the ground. The straight line connecting the UAV and the ground point P is given by,

$$\frac{x}{x - r_0\cos(\phi_0)} = \frac{y}{y - r_0\sin(\phi_0)} = \frac{z - h_0}{z} \tag{12}$$

from which, we can derive the altitude of each point on the LOS link as:

$$z = f(r_0, \phi_0) = h\left(1 - \frac{r\sin(\phi)}{r_0\sin(\phi_0)}\right) \tag{13}$$

In order to efficiently utilize the DTM data, we discretize the virtual altitude z with step size Δz. Next, we can compare the values $k\Delta z$ for $k = 0, \dots, \frac{z}{\Delta z}$ with the practical elevation of environment obstacles obtained from DTM. We define the following indicator function for the generic ground point $P = (0, r_0, \phi_0)$:

$$I(r_0, \phi_0) = \begin{cases} 0 & \text{if } \exists k \big| k\Delta f(r_0, \phi_0) \in \text{DTM} \\ 1 & \text{O.W.} \end{cases}$$

The indicator function determines whether any point of the LOS link is registered on the DTM. In other words, $I(r_0, \phi_0) = 1$ indicates a clear LOS link towards the point P, $I(r_0, \phi_0) = 0$ shows a blocked LOS view. Note that the smaller the value of step size Δz, the more accurate is the output of the indicator function.

Assuming that the radius of raw coverage area of a UAV hovering at altitude h with transmit power P^t is $R(h, P^t)$, the actual mmWave coverage area of the UAV can be computed as

$$A(h) = \int_0^{2\pi} \int_0^{R(h,P^t)} I(r, \phi) r dr d\phi \tag{14}$$

in which R is the radius of coverage circle in the absence of environmental obstacles. Note that if $I(r_0, \phi_0) = 1$, $\forall r_0 \geq 0$, and $\forall 0 \leq \phi_0 \leq 2\pi$, then $A(h) = \pi R^2$, which is the maximum attainable coverage area at altitude h.

Note that due to the practical limitations on the UAV altitude, we have $h_{\min} < h < h_{\max}$. The optimal altitude for maximum mmWave coverage area can be found as,

$$h^* = \underset{h_{\min}<h<h_{\max}}{\text{argmax}} A(h) \tag{15}$$

V. Simulation Results

For simulations, we consider a 10 Km $\times$ 10 Km operation area where the UAVs communicate over 30 GHz carrier frequency in an urban environment with parameters $\alpha = 9.61$, $\beta = 0.16$, and $(\eta_{LOS}, \eta_{NLOS})$ = (1 dB, 20 dB) [24]. We assume that the minimum allowable received signal power for a successful transmission is $\epsilon = -60$ dBm. We also consider a repository of 16 UAVs in which there are four different types of UAVs with maximum transmit powers of 35 dBm, 39 dBm, 43 dBm, and 50 dBm and there are four identical UAVs of each kind. The flight altitude ranges between 400 m and 4000 m.

Figure 2 illustrates the optimal resource allocation and 3D placement of the UAVs for providing maximum coverage without inter-cell interference in the area of interest. It can be seen that only 13 UAVs out of the 16 available UAVs are deployed in the area since deploying more UAVs would unavoidably cause an interference. Indeed, only a single UAV with transmit power 43 dBm is employed while the UAVs in other groups are all utilized.

Figure 3 shows the users' average received data rate versus the number of users for two different distribution models for the users. According to Figure 3, the average received data rate for a given number of users is significantly lower in hotspot areas (i.e., the truncated Gaussian distribution). This is in fact due to the severe blockage caused by the neighboring obstacles located in the hotspot area compared to the more distant and uniformly distributed user scenario in which more users have a chance of LOS connection towards the UAVs.

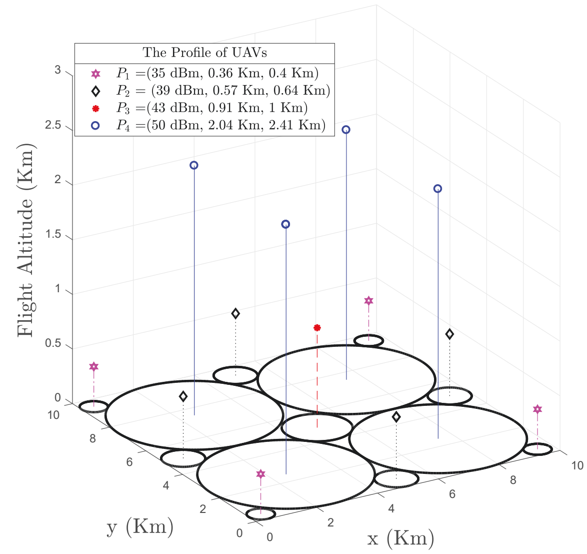

Fig. 2: The optimal 3D placement of the UAVs for maximum coverage area while avoiding inter-cell interference.

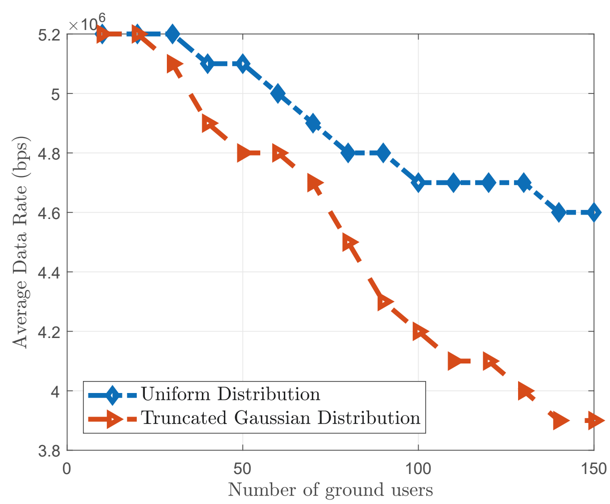

Fig. 3: The deployment of the heterogeneous repository of the UAVs to provide service for ground users for two different distributions

Figure 4 shows the coverage percentage and the number of deployed UAVs as a function of the network size for a square area. Clearly, the number of deployed UAVs is not a monotonically increasing function of the size of area. This is due to the heterogeneity of UAVs and the disparity between their coverage radii. Interestingly, based on the available UAVs in the repository, the maximum coverage percentage is achieved for a 10 Km $\times$ 10 Km area using only 13 UAVs. However, as the side length of the area increases to 11 Km, all the 16 UAVs can be deployed without any inter-cell interference. Therefore, increasing the side length beyond 11 Km accentuates the resource deficiency as the coverage percentage monotonically decreases. This arrangement of the

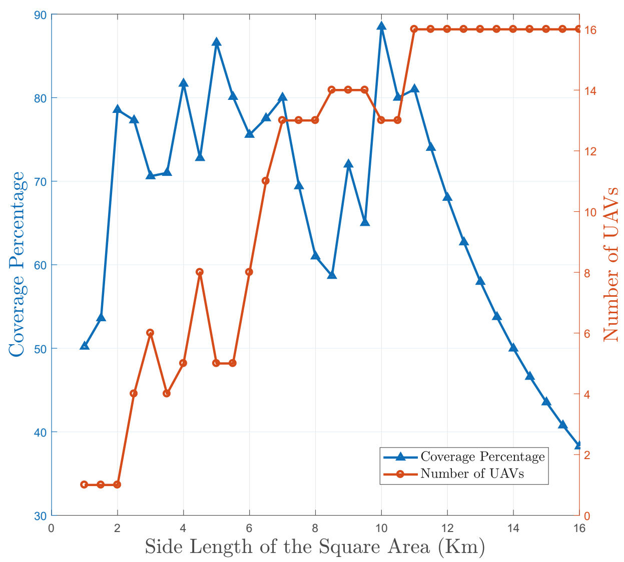

Fig. 4: The coverage percentage and the number of deployed UAVs for different network sizes.

UAVs is the optimal arrangement satisfying the constraints in (6)-(9) and yields 71.54% coverage area.

VI. Conclusion

This paper developed an effective method for resource allocation and optimal 3D placement of a set of heterogeneous UAVs acting as flying mmWave base stations to provide wireless coverage for ground users in an area. First, considering the statistical model of the environment, we derived the optimal horizontal location of the UAVs to maximize the raw coverage area. Then, in order to enable seamless mmWave connectivity, we proposed a geometrical solution to optimize the altitude of UAVs based on the exact realization of environmental parameters. The developed method addresses an important challenge facing the large scale adoption of mmWave for outdoor usage. Finally, simulation results show the effectiveness of the developed 3D cell-planning and performance of the proposed algorithm.

Acknowledgement

This material is based upon work supported by the Air Force Office of Scientific Research under award number FA9550-20-1-0090 and the National Science Foundation under Grant Numbers CNS-2034218, CNS-2204445, and ECCS-2030047.

References

[1] J. Zhang, X. Ge, Q. Li, M. Guizani, and Y. Zhang, "5G millimeter-wave antenna array: design and challenges," *IEEE Wireless communications*, vol. 24, no. 2, pp. 106–112, 2016.

[2] T. S. Rappaport, S. Sun, R. Mayzus, H. Zhao, Y. Azar, K. Wang, G. N. Wong, J. K. Schulz, M. Samimi, and F. Gutierrez, "Millimeter wave mobile communications for 5G cellular: It will work!" *IEEE access*, vol. 1, pp. 335–349, 2013.

[3] W. Saad, M. Bennis, M. Mozaffari, and X. Lin, *Wireless Communications and Networking for Unmanned Aerial Vehicles*. Cambridge University Press, 2020.

[4] E. Vinogradov, H. Sallouha, S. De Bast, M. M. Azari, and S. Pollin, "Tutorial on UAV: A blue sky view on wireless communication," *arXiv preprint arXiv:1901.02306*, 2019.

[5] M. Mozaffari, W. Saad, M. Bennis, Y. Nam, and M. Debbah, "A tutorial on UAVs for wireless networks: Applications, challenges, and open problems," *IEEE Commun. Surveys Tutorials*, vol. 21, no. 3, pp. 2334–2360, 2019.

[6] A. Orsino, A. Ometov, G. Fodor, D. Moltchanov, L. Militano, S. Andreev, O. N. Yilmaz, T. Tirronen, J. Torsner, G. Araniti *et al.*, "Effects of heterogeneous mobility on D2D-and drone-assisted mission-critical MTC in 5G," *IEEE Commun. Mag.*, vol. 55, no. 2, pp. 79–87, 2017.

[7] M. M. Azari, F. Rosas, K. Chen, and S. Pollin, "Optimal UAV positioning for terrestrial-aerial communication in presence of fading," in *Proc. IEEE Glob. Commun. Conf. (GLOBECOM)*, Dec. 2016, pp. 1–7.

[8] A. Al-Hourani, S. Kandeepan, and S. Lardner, "Optimal LAP altitude for maximum coverage," *IEEE Wireless Commun. Lett.*, vol. 3, no. 6, pp. 569–572, Dec. 2014.

[9] M. Mozaffari, W. Saad, M. Bennis, and M. Debbah, "Drone small cells in the clouds: Design, deployment and performance analysis," in *in Proc. IEEE Glob. Commun. Conf. (GLOBECOM)*, San Diego, CA, USA, Dec. 2015, pp. 1–6.

[10] ——, "Efficient deployment of multiple unmanned aerial vehicles for optimal wireless coverage," *IEEE Communications Letters*, vol. 20, no. 8, pp. 1647–1650, 2016.

[11] R. I. Bor-Yaliniz, A. El-Keyi, and H. Yanikomeroglu, "Efficient 3-D placement of an aerial base station in next generation cellular networks," in *Proc. IEEE Int. Conf. on Commun. (ICC)*, May 2016, pp. 1–5.

[12] E. Kalantari, H. Yanikomeroglu, and A. Yongacoglu, "On the number and 3D placement of drone base stations in wireless cellular networks," in *in Proc. IEEE 84th Veh. Techno. Conf. (VTC-Fall)*, Nanjing, China, May 2016, pp. 1–6.

[13] Y. Y. Munaye, H.-P. Lin, A. B. Adege, and G. B. Tarekegn, "UAV positioning for throughput maximization using deep learning approaches," *Sensors*, vol. 19, no. 12, p. 2775, 2019.

[14] X. Liu, Y. Liu, and Y. Chen, "Reinforcement learning in multiple-UAV networks: Deployment and movement design," *IEEE Trans. on Vehicular Technology*, vol. 68, no. 8, pp. 8036–8049, 2019.

[15] D. Orfanus, E. P. de Freitas, and F. Eliassen, "Self-organization as a supporting paradigm for military UAV relay networks," *IEEE Communications Letters*, vol. 20, no. 4, pp. 804–807, 2016.

[16] M. Mozaffari, W. Saad, M. Bennis, and M. Debbah, "Unmanned aerial vehicle with underlaid device-to-device communications: Performance and tradeoffs," *IEEE Trans. on Wireless Commun.*, vol. 15, no. 6, pp. 3949–3963, 2016.

[17] A. Kumbhar, H. Binol, S. Singh, I. Guvenc, and K. Akkaya, "Heuristic approach for jointly optimizing FeICIC and UAV locations in multi-tier LTE-advanced public safety HetNet," *IET Communications*, Sep. 2020.

[18] N. Namvar, A. Homaifar, A. Karimoddini, and B. Maham, "Heterogeneous UAV cells: An effective resource allocation scheme for maximum coverage performance," *IEEE Access*, vol. 7, pp. 164 708–164 719, 2019.

[19] L. Zhang, H. Zhao, S. Hou, Z. Zhao, H. Xu, X. Wu, Q. Wu, and R. Zhang, "A survey on 5g millimeter wave communications for uav-assisted wireless networks," *IEEE Access*, vol. 7, pp. 117 460–117 504, 2019.

[20] Z. Xiao, P. Xia, and X.-G. Xia, "Enabling UAV cellular with millimeter-wave communication: Potentials and approaches," *IEEE Communications Magazine*, vol. 54, no. 5, pp. 66–73, 2016.

[21] B. Li, Z. Fei, and Y. Zhang, "UAV communications for 5G and beyond: Recent advances and future trends," *IEEE Internet of Things Journal*, vol. 6, no. 2, pp. 2241–2263, 2018.

[22] J. Sabzehali, V. K. Shah, H. S. Dhillon, and J. H. Reed, "3D placement and orientation of mmWave-based UAVs for guaranteed LoS coverage," *IEEE Wireless Commun. Letters*, 2021.

[23] M. Boschiero, M. Giordani, M. Polese, and M. Zorzi, "Coverage analysis of UAVs in millimeter wave networks: A stochastic geometry approach," in *2020 International Wireless Communications and Mobile Computing (IWCMC)*, 2020, pp. 351–357.

[24] A. Al-Hourani, S. Kandeepan, and A. Jamalipour, "Modeling air-to-ground path loss for low altitude platforms in urban environments," in *Proc. IEEE Glob. Commun. Conf. (GLOBECOM)*, 2014, pp. 2898–2904.

[25] K. Stephenson, *Introduction to circle packing: The theory of discrete analytic functions*. Cambridge Univ. Press, 2005.